

## Surface and core electronic structure of oxidized silicon nanocrystals

Noor A. Nama<sup>1</sup>, Mudar A. Abdulsattar<sup>2</sup>, Ahmed M. Abdul-Lettif<sup>1</sup>

<sup>1</sup>Physics Department, College of Science, University of Babylon, Babylon, Iraq  
<sup>2</sup>Ministry of Science and Technology, Directorate of Materials Science, Baghdad, Iraq

Ab initio restricted Hartree-Fock method within the framework of large unit cell formalism is used to simulate relatively large silicon nanocrystals between 216 and 1000 atoms that include Bravais and primitive cell multiples. The investigated properties include oxidized surface and core properties. Results revealed that electronic properties converge to some limit as the size of the nanocrystal increases. Increasing the size of the core of a nanocrystal resulted in an increase of energy gap, valence band width, and cohesive energy. The lattice constant of the core and oxidized surface parts show a decreasing trend as the nanocrystal increases in size that converges to 5.28 Å. Surface and core convergence to the same lattice constant reflects good adherence of oxide layer at the surface. The core density of states shows a highly degenerate states that split at the oxygenated (001)-(1×1) surface due to symmetry breaking. The nanocrystal surface shows smaller gap, higher valence and conduction bands when compared to the core part due to oxygen surface atoms and reduced structural symmetry. Nanocrystal geometry proved to have strong influence on all electronic properties including the energy gap.

### I. Introduction

Silicon has many industrial uses and is considered one of the most important semiconductors [1]. It is the principal component of most semiconductor devices, most importantly integrated circuits. Silicon is widely used in semiconductors because it remains a semiconductor at higher temperatures than the semiconductor germanium and because its native oxide forms a better semiconductor/dielectric interface than any other material. The applications of silicon are in the electronic current conduction control (transistors), IC, detectors, solar cells ...etc. Nanocrystalline silicon (nc-Si) has small grains of crystalline silicon within the amorphous phase (a-Si). One of the most important advantages of nanocrystalline silicon, is that it has increased stability over (a-Si).

Silicon has been studied extensively because it is widely used in electronic products [1-6]. On the other hand, the investigation of silicon nanocrystals is still an active field for investigation [3-6]. Silicon nanocrystals electronic structure of small hydrogenated or oxidized nanocrystals typically less than 500 atoms is recently performed using ab initio methods in the last years [3-6]. The present work addresses larger nanocrystals that have the size range of 216-1000 silicon atoms. The present upper

limit size has not been investigated before using ab initio methods that requires long execution computer times and higher memory which is the case of the present work.

Large unit cell method (LUC) coupled with ab initio Hartree-Fock electronic structure calculations are used in the present work. LUC method was formulated and used before for several kinds of bulk materials including diamond structured materials [6-9]. Semiempirical LUC calculations were performed previously for silicon nanocrystals [10] with smaller number of atoms. The sizes covered in this work include cubic and parallelepiped nanocrystals that have lengths from 1.6 to 2.7 nm (216 to 1000 atoms).

## II. Theory

Ab initio self-consistent Hartree-Fock is used to obtain silicon nanocrystal molecular orbitals. Correlation corrections are neglected in the present calculations relying on Koopmans theorem [11]. This theorem states that comparisons of Hartree-Fock closed shell results (which is the case in the present work) with experimental values suggest that in many cases the energetic corrections due to relaxation effects nearly cancel the corrections due to electron correlation

In the present work, we divided calculations into two parts; core and surface part which is the traditional method used in microscopic size solid state calculations. Normally surface effects do not penetrate more than four layers of the crystal surface [12]. On the other hand, short range  $sp^3$  bonds in diamond structured elements do not require more than fourth neighbor's interaction range to conduct electronic structure calculations successfully [8-10]. The upper two identical conditions will be applied in the present calculations. Previous silicon nanocrystals surface calculations [3, 5, 14] showed that double bonding (Si=O) of oxygenated surfaces is preferred on single bridge bonding (Si-O-Si). Many reasons might support this bonding such as surface curvature and larger lattice constants and bond lengths of nanocrystals. As a consequence of the above mentioned reasons, the oxygen atoms are found in the vicinity of one silicon atom and far enough from other silicon surface atoms that promote double oxygen bonding.

Two kinds of core LUCs are investigated, namely cubic and parallelepiped cells. The cubic cells are multiples of diamond structure Bravais unit cells, while the parallelepiped cells are multiples of primitive diamond structure unit cells [12]. Cubic core cells include 8, 64, 216 atoms. Parallelepiped cells include 16, 54, and 128 atoms.

## III. Calculations and results

We shall perform the core part calculations using 3D large unit cell method (LUC). The 2D calculations for the oxygenated (001)-(1×1) surface is added to obtain a complete electronic structure view. The periodic boundary condition (PBC) method available in GUSSIAN 03 program [13] is used to perform the present tasks.

In Fig. 1 total energy of 216 Si atoms nanocrystal core as a function of lattice constant is plotted. This curve and similar curves for other LUCs are used to obtain equilibrium lattice constants for these cells. Fig. 2 shows the equilibrium lattice constants obtained from the previous curves plotted against number of core atoms. Energy gap, valence band width and cohesive energy are plotted against the number of core atoms in Figs. (3-5) respectively.

Three periodic slab stoichiometries were investigated to examine oxygenated (001)-(1×1) surface namely  $Si_{16}O_4$ ,  $Si_{64}O_{16}$ , and  $Si_{144}O_{36}$ . These stoichiometries have surface areas

$a^2$ ,  $4a^2$ , and  $9a^2$  respectively ( $a$  is the lattice constant). Fig. 6 shows the surface energy gap of the oxygenated (001)-(1×1) surface as a function of surface area of Si nanocrystal facet. This figure is followed by a comparison between core and surface density of states in Fig. 7. A batman shape curve of ionic charges in oxygenated (001)-(1×1) surface of periodic  $\text{Si}_{16}\text{O}_4$  stoichiometry is shown in Fig. 8.

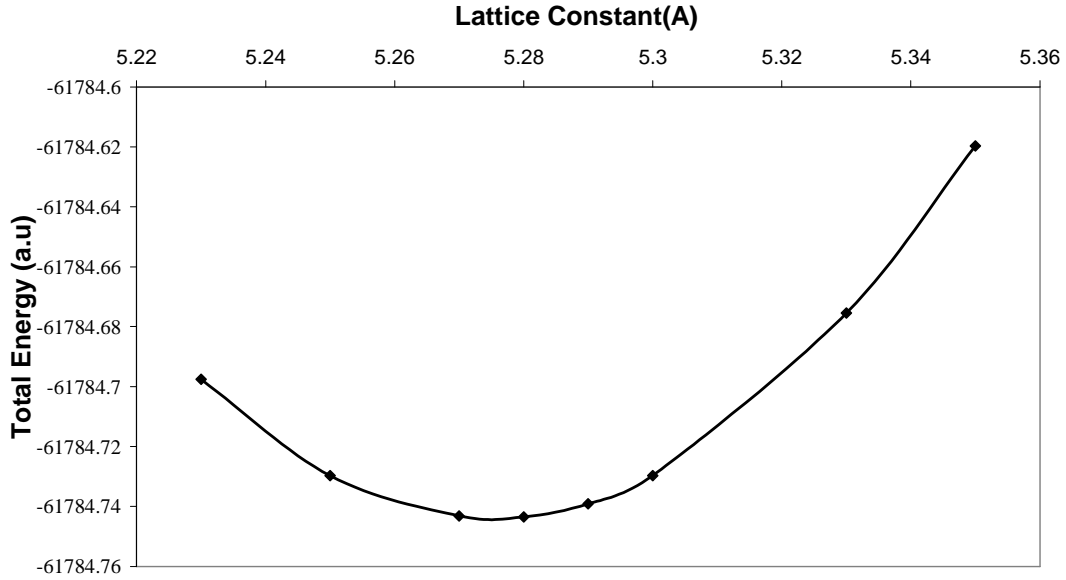


**Fig. 1** Total energy of 216 Si atom nanocrystal core as a function of lattice constant.

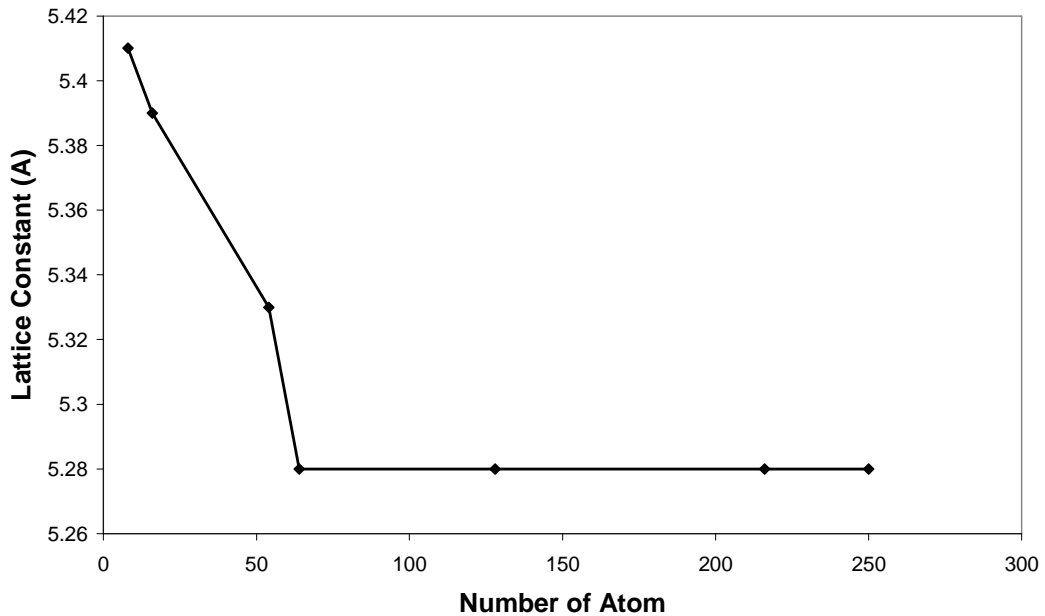


**Fig. 2** Lattice constant as a function of number of core atoms for Si nanocrystal.

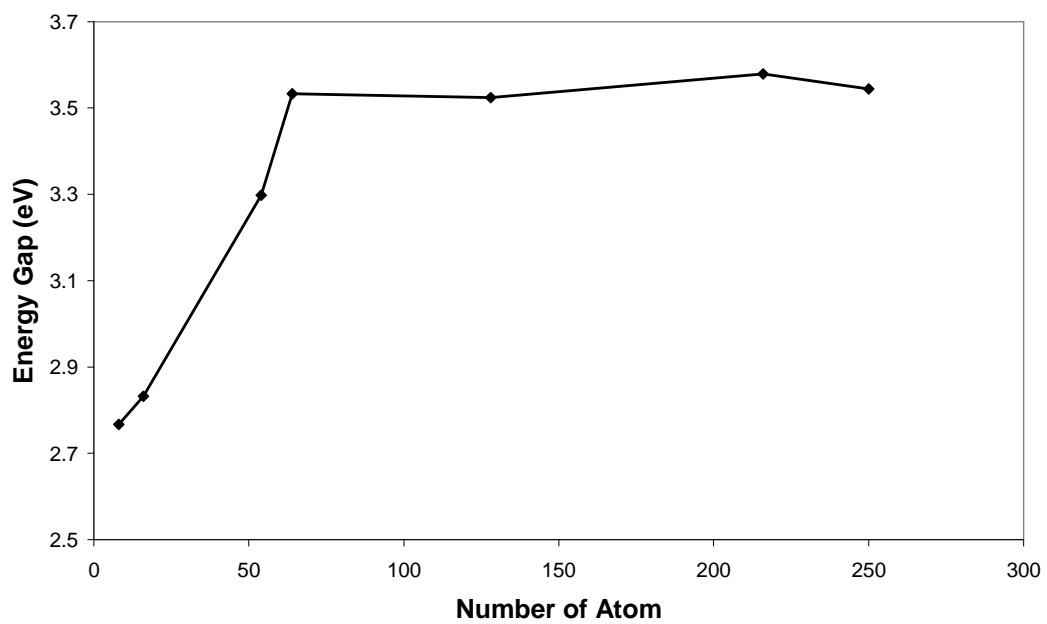


**Fig. 3** Energy gap of Si nanocrystal core as a function of number of atoms.

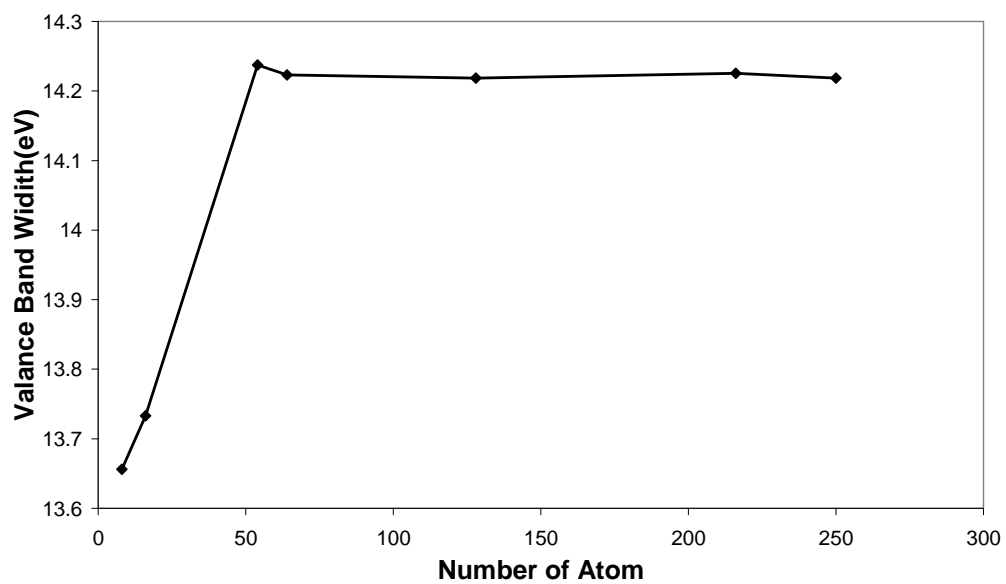


**Fig. 4** Valance band width of Si nanocrystals core as a function of number of atoms.

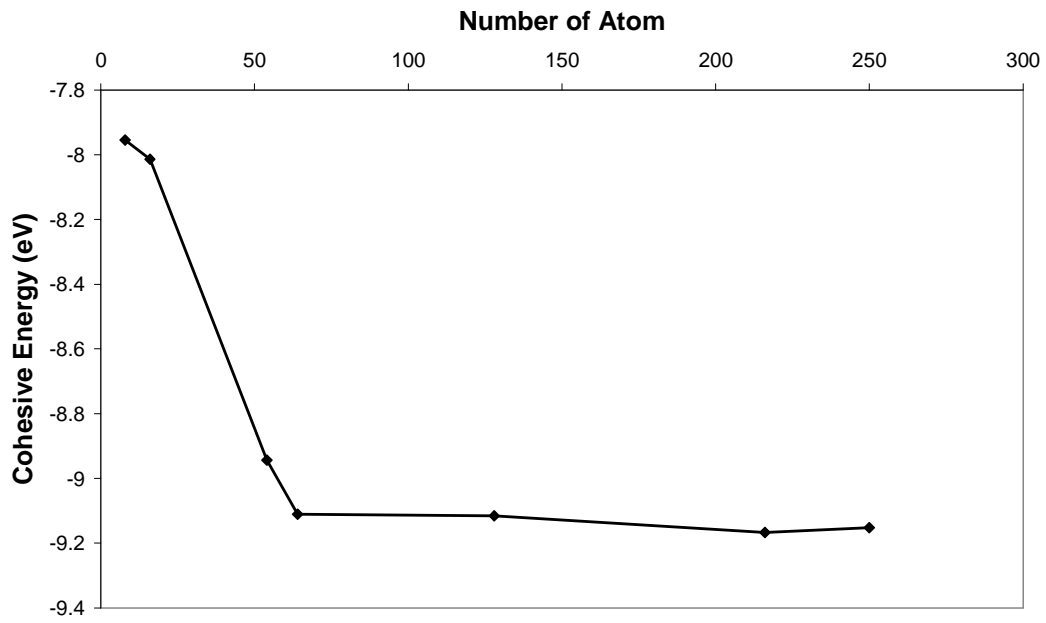


**Fig. 5** Cohesive energy for Si nanocrystal core as a function of number of atoms.

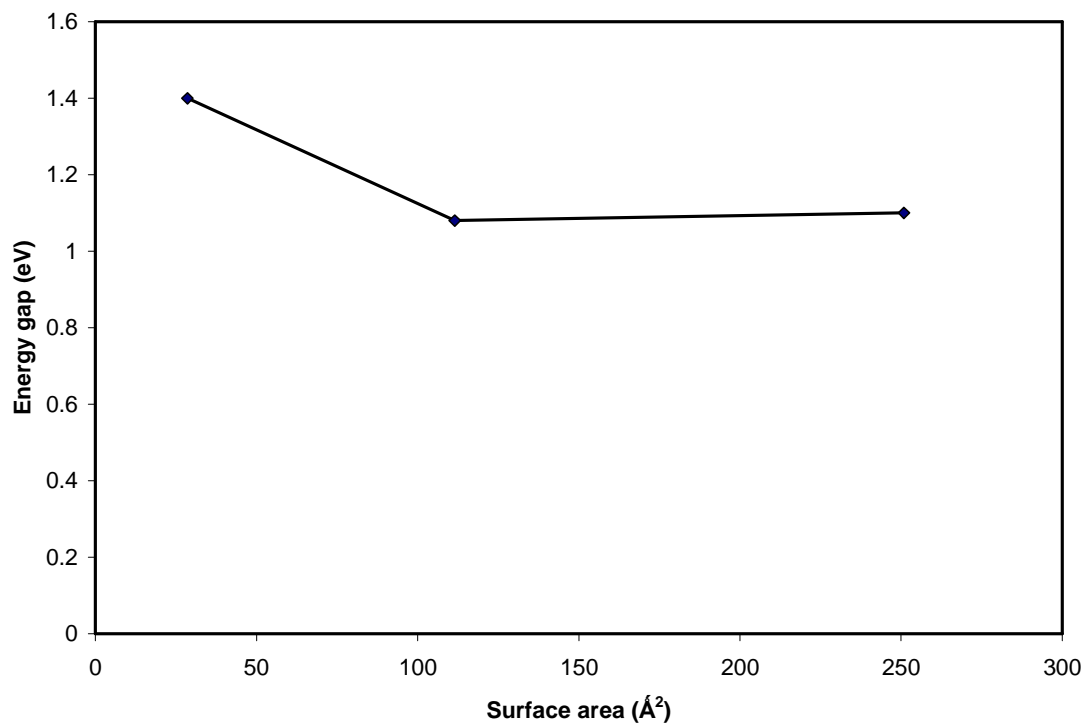
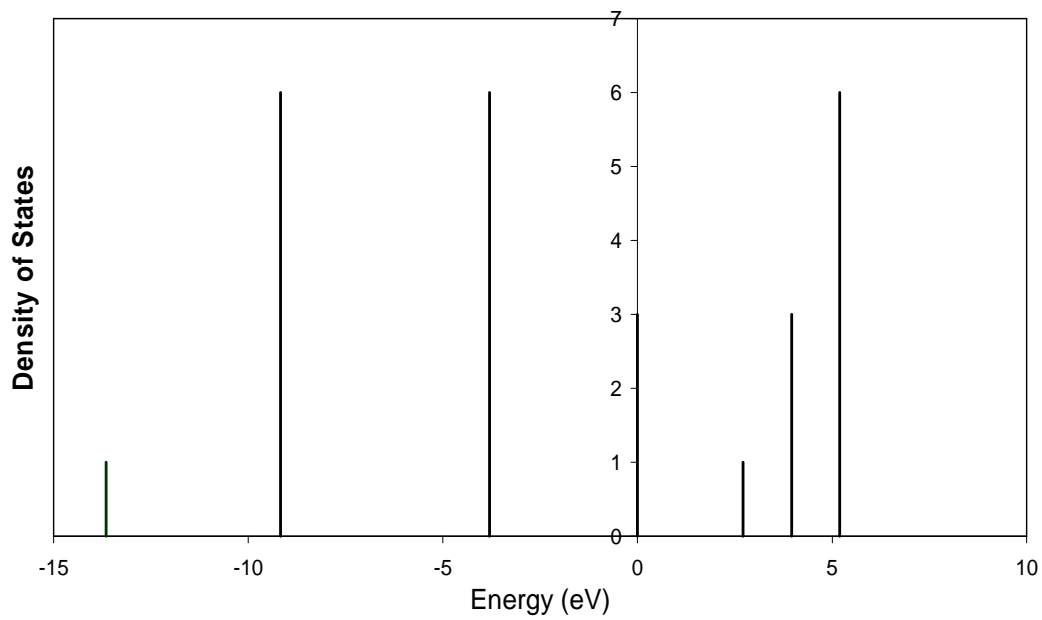
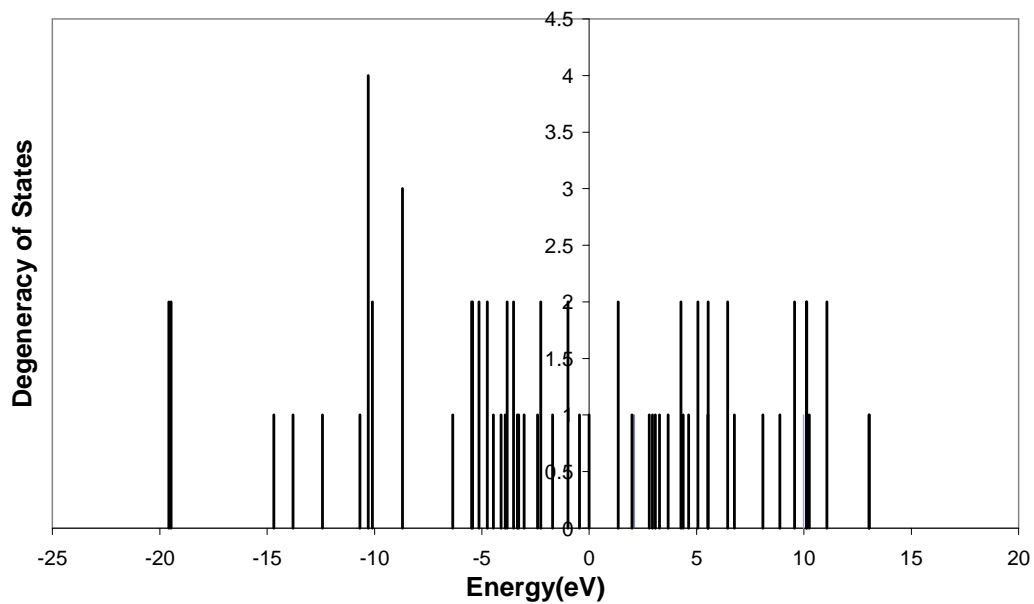


**Fig. 6** Energy gap of Si nanocrystal oxygenated (001)-(1×1) face as a function of surface area of nanocrystal facet.



(a)



(b)

**Fig. 7** Degeneracy of states of 8 atoms LUC as a function of levels energy (a), and (b) surface density of states of oxygenated (001)-(1x1) slab with  $a^2$  surface area.

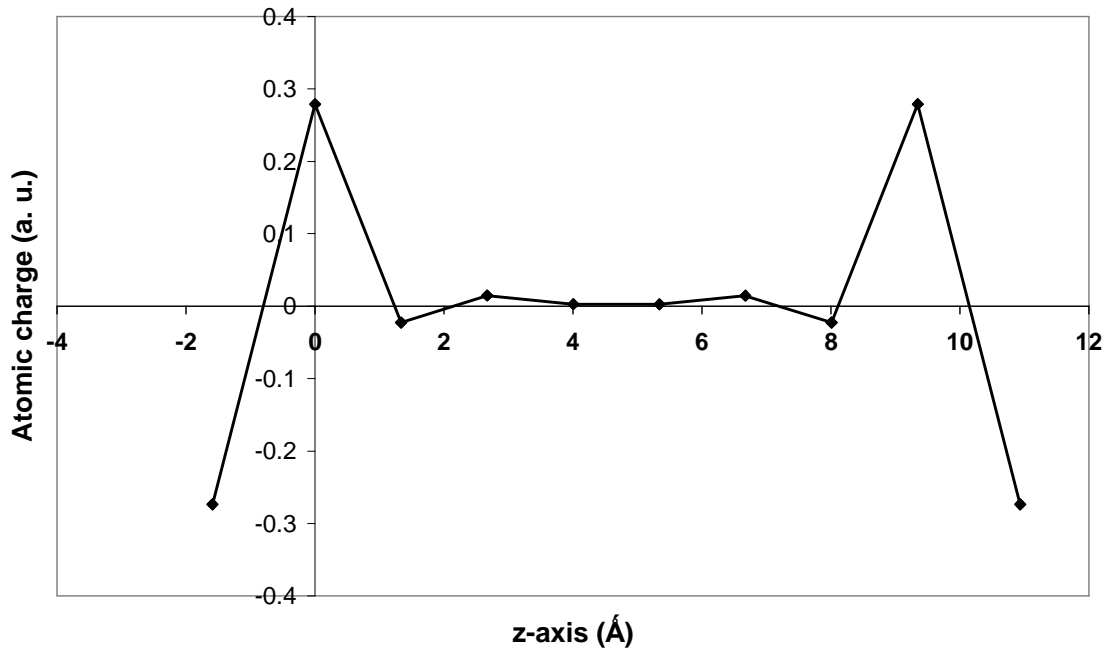


**Fig. 8** Ionic charges of oxygenated (001)-(1x1) surface slab calculations as a function of layer depth.

#### IV. Discussion and conclusions

Because of symmetry the core part has a unique single structure. This is the opposite case of surface multiple structures in which orientation, passivating atoms and other situations in which surface structure changes accordingly. Fig. 1 shows the variation of lattice constant with the number of core atoms. The variation of lattice constant is all what we need to assign the equilibrium geometry for the core part. The group of equilibrium constants for each of the investigated core sizes is plot against the number of atoms in Fig. 2. This figure shows that core lattice constant converge to some value as the nanocrystal grow up in size. This value is 5.28 Å which is in a good agreement with the experimental value 5.43 Å [1]. Surprisingly, the oxygenated (001)-(1×1) surface slab calculations of the nanocrystal converges to approximately the same lattice constant value of the core (5.28 Å). This shows that negligible stresses are encountered at the interface between surface and core parts which eventually reflects good adherence of the oxide layer.

Energy gap, valence band width and cohesive energy of the core part that are plotted against the number of core atoms in Figures (3-5) respectively, show a converging behavior as the number of core atoms increases. This convergence is associated with fluctuations depending on the geometry of the nanocrystal core. At the convergence plateau Bravais cubic lattices seems to have higher energy gaps, valence band width, and cohesive energy (absolute value). This is a clear indication of geometry effects on electronic structure of nanocrystals. Energy gap is inversely proportional to the surface area of core atoms. Parallelepiped cells have less gap values than cubic ones. This

discrimination between the electronic properties is also applicable to cohesive and valence band energies. These differences diminish as the nanocrystal grows up in size.

Figure 6 shows the energy gap of oxygenated (001)-(1x1) silicon surface. From comparison of this figure with Fig. 3, we can note that energy gap at the surface is much less than that at core. As a consequence, the energy gap is controlled by the surface of nanocrystals. The descending energy gap shape of Fig. 6 leads to the result that silicon nanocrystals at this size obey quantum confinement implications. Experimentally Measured energy gap of silicon nanocrystals with a mean size of 4 nm embedded in a SiO<sub>2</sub> matrix is 1.7 eV [15]. Although the size and matrix is different than the present calculations, the present surface gap result (1.1 eV) shows good agreement with experiment. Hydrogenated silicon nanocrystals [16, 17] show higher band gaps than oxygenated silicon nanocrystals. Surface modification by different atoms is discussed in reference [18]. The oxygen double bonding to the surface seems to be also favorable in silicon nanocrystals interface and small nanocrystals [19, 20].

Mesoscopic thermal conductance fluctuations of silicon nanowires are measured in reference [21]. The present fluctuations seem to be originating from different geometrical origin, although fluctuations in conductance should also occur in the present case due to fluctuations in the energy gap [1]. The present results are related to size and geometry which is far from the size of reference [21] ( $200 \times 100 \text{ nm}^2$  cross-section).

Fig. 7 shows a comparison between surface and bulk density of states. Zero energy is assigned to the highest occupied molecular orbital (HOMO). In this figure we can notice that degeneracy of states is reduced in surface case due to splitting of these states. As a consequence of this splitting, the band gap is decreased and valence and conduction bands are increased.

Fig. 8 shows the surface ionic charges of oxygenated (001)-(1x1) surface slab as a function of layer depth. The first and last atoms in the figure are for oxygen atoms which have negative charges due to their high affinity. Silicon atoms that are adjacent to oxygen atoms have positive charges. The second silicon neighbors to oxygen atoms have negative charges while the third neighbors have positive charges. This damping oscillatory charges ends at the fourth neighbors with practically zero charge. This curve is a good proof for the previously mentioned postulate of the adequacy of using four layers to represent the surface.

Empirical or semiempirical methods that neglect large amount of the exact ab initio theory also exist and applied to silicon nanocrystals [10, 22]. These methods fit their empirical parameters to the available experimental data. These methods can simulate thousands of atoms at reasonable times. However, these models can be considered as a first approximation for the determination of the anticipated accurate structures using ab initio methods [13].

Summarizing the upper mentioned conclusions: the core part has a converging fluctuating energy gap, valence band width and cohesive energy. These fluctuations are related to the geometry of the nanocrystal. The energy gap is controlled by the surface part of the nanocrystal with the surface having damping oscillatory successive negative and positive layer charges. The surface part has lower symmetry than the core part with smaller energy gap and wider valence and conduction bands. Surface and core parts have approximately the same lattice constant that reflects the good adherence of oxide layer at the surface.

- [1] S. M. Sze and K. K. Ng, *Physics of semiconductor devices*, 3<sup>rd</sup> edition, Wiley (2007).
- [2] S. J. Clark and G. J. Ackland, *Phys. Rev. B* **48**, 10899 (1993).
- [3] M. Luppi and S. Ossicini, *Phys. Rev. B* **71**, 035340 (2005).
- [4] T. van Buuren, L.N. Dinh, L.L. Chase, W.J. Siekhaus, L.J. Terminello, *Phys. Rev. Lett.* **80**, 3803 (1998).
- [5] P. Carrier, *Phys. Rev. B* **80**, 075319 (2009).
- [6] Mudar A. Abdulsattar, Khalil H. Al-Bayati, *Phys. Rev. B* **75**, 245201 (2007).
- [7] R. Evarestov, M. Petrashen, E. Lodovskaya, *Phys. Status Solidi b* **68**, 453 (1975).
- [8] A. Harker, F. Larkins, *J. Phys. C* **12**, 2487 (1979).
- [9] A. Harker, F. Larkins, *J. Phys. C* **12**, 2497 (1979).
- [10] Mudar A. Abdulsattar, *Physica E* **41**, 1679 (2009).
- [11] W. Hehre L. Radom, P. Schleyer, and J. Pople, *Ab Initio Molecular Orbital Theory* \_Wiley, New York 1986\_.
- [12] C. Kittel, *Introduction to Solid State Physics*, 5th edition, Wiley, (1976).
- [13] Gaussian 03, Revision B.01, M. J. Frisch, G. W. Trucks, H. B. Schlegel, G. E. Scuseria, M. A. Robb, J. R. Cheeseman, J. A. Montgomery, Jr., T. Vreven, K. N. Kudin, J. C. Burant, J. M. Millam, S. S. Iyengar, J. Tomasi, V. Barone, B. Mennucci, M. Cossi, G. Scalmani, N. Rega, G. A. Petersson, H. Nakatsuji, M. Hada, M. Ehara, K. Toyota, R. Fukuda, J. Hasegawa, M. Ishida, T. Nakajima, Y. Honda, O. Kitao, H. Nakai, M. Klene, X. Li, J. E. Knox, H. P. Hratchian, J. B. Cross, C. Adamo, J. Jaramillo, R. Gomperts, R. E. Stratmann, O. Yazyev, A. J. Austin, R. Cammi, C. Pomelli, J. W. Ochterski, P. Y. Ayala, K. Morokuma, G. A. Voth, P. Salvador, J. J. Dannenberg, V. G. Zakrzewski, S. Dapprich, A. D. Daniels, M. C. Strain, O. Farkas, D. K. Malick, A. D. Rabuck, K. Raghavachari, J. B. Foresman, J. V. Ortiz, Q. Cui, A. G. Baboul, S. Clifford, J. Cioslowski, B. B. Stefanov, G. Liu, A. Liashenko, P. Piskorz, I. Komaromi, R. L. Martin, D. J. Fox, T. Keith, M. A. Al-Laham, C. Y. Peng, A. Nanayakkara, M. Challacombe, P. M. W. Gill, B. Johnson, W. Chen, M. W. Wong, C. Gonzalez, and J. A. Pople, Gaussian, Inc., Pittsburgh PA, (2003).
- [14] I Vasiliev, J. R. Chelikowsky, and R. M. Martin, *Phys. Rev. B* **65**, 121302(R) (2002).
- [15] L. Ding, T. P. Chen, Y. Liu, C. Y. Ng, and S. Fung, *Phys. Rev. B* **72**, 125419 (2005).
- [16] I. Vasiliev, S. Ögüt, and J. R. Chelikowsky, *Phys. Rev. Lett.* **88**, 097401 (2002).
- [17] Z. Zhou, R. A. Friesner, and L. Brus, *J. Am. Chem. Soc.* **125**, 15599 (2003).
- [18] A. Puzder, A. J. Williamson, J. C. Grossman, and G. Galli, *Phys. Rev. Lett.* **88**, 097401 (2002).
- [19] X. Chen, X. Pi, and D. Yang, *J. Phys. Chem. C* **114**, 8774 (2010).
- [20] R. J. Eyre, J. P. Goss, and P. R. Briddon, *Phys. Rev. B* **77**, 245407 (2008).
- [21] J. S. Heron, T. Fournier, N. Mingo, and O. Bourgeois, *Nano Lett.* **9**, 1861 (2009).
- [22] C. Bulutay, *Phys. Rev.* **76**, 205321 (2007).